Version	**Description**	**Changed By**	**Date**
1.0	First draft	A. Polebitski	07/09/11

1 Index

2 Problem Statement

The purpose of this work is to provide a flexible and scalable framework to assess the impacts of climate change on streamflow and stream temperature within the North Atlantic Landscape Conservation Cooperative (NALCC) region (Figure 1). The framework must formally address uncertainty in the modelling approach and future climate changes. The framework should replicate seasonal streamflow and temperature patterns for many watersheds within the NALCC.

Index

3 Solution Statement

Forecasting the impacts of land use and climate change on stream hydrology and temperature throughout the NALCC requires a flexible and scalable approach. The approach selected must adequately capture the impacts of non-stationary exogenous variables (air temperature, precipitation, and land use, among other factors) on hydrologic processes, be transferable to multiple watersheds with minimal effort, and provide quantified and easily communicated measures of uncertainty. In addition, innovative methods are required to characterize the uncertainty of model estimates where there is a paucity of observed data for calibration. This work will produce physically-based hydrologic models that satisfy all of these requirements and contribute to the development of a hydrologic modelling methodology that can be extended to the entire NALCC region.

We use the ABCD hydrology model to generate streamflow and a nonlinear model developed by Mohseni et al. (1999) to simulate streamflow and stream. The hydrology model generates monthly streamflow values while the stream temperature model produces weekly stream temperature results. Both models are formulated in a hierarchical Bayesian framework to account for parameter uncertainty. Monte Carlo Markov Chain resamling is used to explore the parameter space of model parameters and identify their most likely distributions, allowing model uncertainty to be formally quantified. Parameters are also allowed to vary by basin characteristics, enabling the development of relationships that can inform model development in ungaged watersheds. Our approach will use the World Climate Research Programme's (WCRP's) Coupled Model Intercomparison Project phase 3 (CMIP3) multi-model dataset as the foundation for the climate change analysis. These data provide a gridded dataset of downscaled monthly temperature and precipitation projections for 112 IPCC climate change scenarios. This ensemble of climate data is used to categorize and quantify the uncertainty in climate model projections.

Index

4 Key Features

This work is divided into two primary tasks, each with multiple subcomponents. The first task explores the use of a parsimonious hydrologic model for simulating streamflow throughout the NALCC under climate and land use changes. These models will be calibrated in a hierarchical Bayesian framework that combines information of characteristics of each watershed with any and all streamflow data to develop robust and physically meaningful model parameters for watersheds from locations across the NALCC to provide improved model parameter estimates at ungaged locations. The Bayesian framework also allows direct estimation of uncertainty bounds on the streamflow predictions for any location.

The second task of this effort will explore empirical techniques for modelling stream temperature. As with the hydrology model, the stream temperature model will be formulated within a hierarchical Bayesian framework, allowing model parameters to be scalable across space and inferred from basin characteristics. For both the hydrologic and temperature models, uncertainty in model outputs can be directly assessed and propagated through biological models of fish survival.

In accomplishing these two tasks, we will develop and verify a hydrologic and stream temperature model for a set of watersheds in the NALCC. This work will provide a framework to produce parsimonious hydrology models of monthly streamflow and water temperature across the entire NALCC region. In the future we envision this effort contributing to the development of a decision support system that accesses a collection of parsimonious hydrologic models and their predictions of flow and water temperature under future climate and land use scenarios across the entire Northeast United States. The hydrologic data for this decision support system will inform resource managers of potential risks to their ecological systems and provides an accurate accounting of uncertainty to help direct restoration efforts across the region.

4.1 Hydrology Model - ABCD Model

The ABCD model was first formulated by Thomas (1981), and since tested and modified by Alley (1984), Fernandez et al.(2000), and Martinez and Gupta (2010), among others. The ABCD model is broken into two main components: the hydrology model (a, b, c, and d parameters) and the snow model (e,f, and dif parameters). Figure 2 presents a schematic of the underlying model structure, with the dashed box highlighting a snow model component that can be appended to the overall model for watersheds in higher latitudes and elevations. A hierarchical Bayesian framework will be developed and applied to the ABCD model for generalization of the hydrology model to the entire NALCC. The model is currently being developed for a subset of watersheds in the Northeast United States. This document highlights our application of ABCD models and the overall modelling strategy using sub-watersheds within the Connecticut River Basin. Here, we show the model's effectiveness in reproducing streamflow at a monthly time step accurately across a wide range of basins, and the ability to estimate flows in ungaged basins, a challenge still facing the hydrology community. The model's reduced parameter space allows model uncertainty to be explicitly estimated using the Bayesian framework.

Hierarchical Bayesian calibration techniques can be employed to characterize model parameterization in a probabilistic fashion (Bates and Campbell 2001, Marshall 2004), an advantage traditionally available only to statistical models. This Bayesian approach can combine prior belief of model parameter values (expressed as a probability distribution referred to as the prior) with observed data for the study site to produce post-calibration estimates of model parameter probability distributions (i.e. posterior distributions). Previous studies of ABCD model calibration in the Northeast provide a direct source of prior information regarding parameter values (Fernandez et al., 2000, Martinez and Gupta, 2010), and gage data can drive the Bayesian calibration for individual study sites. Figure 3 shows an example of this calibration process, displaying both the prior probability distribution for model parameter "a" and the posterior distribution that results from the incorporation of local watershed data, in this case based on the USGS gage in Huntington MA on the Westfield River. The Bayesian calibration scheme produces a more refined and precise estimate of the model parameter compared to the relatively vague prior information

available before the calibration is performed. Also, the posterior distributions of all model parameters can be propagated through the hydrologic model to produce explicit estimates of streamflow uncertainty. To build the ABCD models, monthly climate data will be collected at each of the study sites and a methodology will be developed to automatically build and calibrate these models for all study sites simultaneously. This methodology can be extended to the entire NALCC region in future work.

4.1.1 Model Details

The ABCD model is a simple hydrology with four parameters (*a, b, c, d*) that dictate water movement through the land surface. In this section we describe the components of the ABCD model and modifications made to improve model behaviour. For this research effort, a snow model is appended to the base model and uses three parameters to govern snow melt and accumulation (Figure 2). In general, the snow model can be thought of as a filter that passes 'effective precipitation' to the ABCD model. The snow model effectively acts as a third storage tank for water during the winter seasons and has no effect on water cycling other times of the year. The ABCD model receives the effective precipitation from the snow model and partitions it to evapotranspiration, runoff, soil moisture, and groundwater flow. The partitioning of the effective precipitation is driven by the monthly meteorological forcing and the model parameters (*a, b, c,* and *d*).

4.1.1.1 ABCD Model Overview

The ABCD model is a conceptual hydrology model capable of replicating monthly water budgets and mean monthly streamflow for many watersheds. The ABCD model represents only the water budgets once water enters the land surface and does not calibrate well in the presence of snow if decoupled from the snow model. The ABCD model has had wide applications in both research (Thomas 1991, Alley 1994, Fernandez 2000, Martinez 2010, and Steinschneider 2011), as well as being incorporated into software packages to serve as the hydrologic component (WEAP).

Figure 2 provides a schematic of the conceptual model and the compartments and parameters governing its 'physics'. In general, precipitation entering the model can enter the stream via direct runoff, outflow from the upper soil zone or a slower outflow from component from the lower soil zone. Potential evapotranspiration is calculated outside of the model and introduced as a forcing, as is precipitation.

Potential evapotranspiration is modified by the snow model, producing what is termed effective evapotranspiration (ET_{eff}). ET_{eff} determines the amount of water that exits the system via actual evapotranspiration (computed as part of the water budget in the ABCD model) and the water that remains in the soil or exits to the stream channel.

The ABCD model consists of four '*calibration parameters*' and five '*state variables*'. *Calibration parameters* are those parameters (*a, b, c, and d*) which govern how water moves between the *state variables* (*W, Y, E, S, and G*) for each time step. Values of *a*, *b*, *c,* and *d* are calibrated and remain static values over a simulation once optimal values are determined. The *state variables* vary over a simulation as variable meteorological forcings are propagated through the model for a given watershed.

The following section is a description of model governing equations, state variables, and calibration parameters. We provide examples of how variation of calibration parameters affects model state variables in Figure 4. The table below (Table 1) lists the values of model inputs, and the values at which calibration parameters were held constant when a single calibration parameter was varied in Figure 4. For instance, the top right pane of Figure 4 plots the values of state variables as calibration parameter *'a'* is varied between the range of 0.70 and 1.0. The change in model outflow is depicted in the top left pane.

State Variables

State Variable 'W'

State variable *W* represents the 'available water' in the system at the current time step. It is defined as $W = P_{eff} + S_{t-1}$, where P_{eff} is the effective precipitation for the current timestep and S_{t-1} is the water stored in the upper soil zone at the end of the previous time step. Variable *W* can be influenced by *b* due to the control *b* has on capacity of the upper soil zone storage. It is also influenced by *a* and *c* through the storage term, *S*. This is not clearly depicted in Figure 4 because the previous time step soil storage is held constant while the calibration parameters were varied.

State Variable 'Y'

State variable *Y* is defined as the evapotranspiration opportunity of the system. It is mathematically defined as: $Y = \frac{W+b}{2a} - \sqrt{\left(\frac{W+b}{2a}\right)^2 - \frac{W*b}{a}}$ Where *W* is the available water in the system for the current time step, and *a* and *b* are model calibration parameters. Evapotransipiration opportunity (*Y*) is nonlinearly related to *W* such that it increases when $W < b$ (water limited conditions) but asymptotically approaches *b* in energy limited conditions ($W \gg b$). The second set of panes in Figure 4 depicts this relationship as parameter *b* is varied between values of 50-800 (completely saturated soil conditions to water limited conditions – initial upper zone water in this example is 50 units). As *b* becomes larger, *Y* quickly approaches the value of *W,* eventually nearing the value of *b*.

State Variable 'S'

Upper zone storage (*S*) is defined mathematically as: $S = Y * e^{-1ET_{eff}*b}$. Total upper zone storage is sensitive to changes in calibration parameter *b*. As *b* increases, available upper zone water storage increases. It is modestly sensitive to parameter *a* through its relationship with state variable *Y*. The top two sets of panes in Figure 4 display how variation in parameter *a* and *b* change *S*. Increases in *a* tend to increase water entering available storage, generating less direct runoff as the water is subjected to evapotranspiration. Increases in parameter *b* increase *S* as *b* represents the size of the upper zone storage, so as *b* increases, more water can be stored in the system.

State Variable 'E'

Total evapotranspiration *E* represents the actual evapotranspiration leaving the system in each time step. Evapotranspiration is specified in the model as: $E = Y * (1 - e^{-1ET_{eff}*b})$. Evapotranspiration is affected be parameter *a* and *b* in similar fashion to parameter *S*, as both share similar functional forms. Increases in *a* tend to slightly increase evapotranspiration, while increases in *b* will decrease *E* as the capacity of the upper soil zone increases, and the ability of water to leave the soil decreases.

State Variable 'G'

Lower soil zone storage (*G*) is governed primarily by calibration parameters *c* and *d*. *G* is unbounded, in that it has infinite storage capacity. Storage in *G* is limited by the different rates at which water enters it from the upper soil zone, and leaves into the stream. As parameter *c* increases, there is a net increase in water present in *G*, as *c* controls the rate at which water moves from the upper soil zone to the lower soil zone. As parameter *d* increases in value, water moves more quickly from the lower soil zone into the stream channel, reducing the value of *G*.

G at time t is given by $G_t = G_{t-1} + c\ W_t - Y_t - d * G_t$. A numeric solution via iteration gives: $G_t = G_{t-1} + \frac{c*(W+Y)}{1+d}$.

<u>Calibration Parameters</u>

Calibration Parameter 'a'

Parameter *a* reflects the 'propensity of runoff to occur before soil is fully saturated' (Thomas et al. 1983). Parameter *a* is bounded between 0 and 1, though typically takes values closer to 1 (Martinez and Gupta 2010, Alley 1984, Fernandez et al. 2000). Parameter *a* is important in calculating *W* (available water) and *Y* (evapotranspiration opportunity). Fernandez et al. (2000) found that parameter *a* is well correlated and explained by soil permeability, with lower permeability soils associated with lower *a* values, and thus lower infiltration into upper soil zone storage and more direct runoff. Increases in parameter *a* with other model parameters held constant tends to decrease overall runoff, as shown in Figure 4 .

Calibration Parameter 'b'

The capacity of the upper soil zone is determined by parameter *b*. It is formally defined as the upper limit of the sum of actual evapotranspiration (*E*) and soil moisture (*S*) within a time step. Parameter *b* is unbounded, but typically takes values between 200 and 600. Increases in parameter *b* tend to increase storage (*S*) and decrease evapotranspiration (*E*), and increase evapotranspiration opportunity (*Y*). Previous work has found permeability of soils within a basin to be strongly related to *b* (Fernandez et al. 2000). Changes in parameter *b* with other model parameters held constant tends to sharply decrease overall runoff.

Calibration Parameter 'c'

Calibration parameter *c* governs the rate at which water moves from the upper soil zone to both the stream and lower soil zone (*G*). Increasing *c* allows more water to be stored as groundwater (*G*). Fernandez et al. (2000) found strong relationships between a metric known as the baseflow index (BFI) and parameter c, as parameter *c* represents the fraction of streamflow that arises from groundwater.

Calibration Parameter 'd'

Groundwater exits model parameter *G* at a rate of calibration parameter *d*. Increasing *d* increases the rate at which water exits *G*, decreasing the water stored in the lower soil zone.

High values of *d* can indicate groundwater dominated streams, and the reciprocal of *d* is equal to the average groundwater residence time for a system (Fernandez et al. 2000). Parameter *d* can be related to baseflow recession constants, as determined by Vogel and Kroll (1996). Parameter *d* is used to calculate water entering *G*, and water entering the stream channel, from deep groundwater storage.

4.1.1.2 Snow Model Overview

The snow model provides one-way interaction with the ABCD model in the form of effective precipitation (the summation of P_t and SM_t in Figure 2) and potential evapotranspiration. In regions with temperature regimes that do not create strong seasonal snow pack, the snow model can be completely decoupled from ABCD. Figure 5 provides an overview of the snow model adopted as part of this work. The parameters *e*, *f*, and *dif* control the rate of melt, the upper bound where snow is present, and the range in which precipitation falls as a mixture of snow and rain. The variables *A*, *mt*, and *frac* represent the accumulation of snowpack, melt water contributing to effective precipitation, and the fraction of total precipitation falling as snow. Figure 6 plots the mass balance of these terms over varying temperature values and static *e*, *f*, and *dif* values. In this example, $e = 0.5$, $f = 2.5$, and $dif = 12.5$, thus the band of *T* where precipitation is mixed between snow and rain lies between 2.5 ˚C and -10 ˚C. The bottom half of Figure 6 displays how *Frac* varies across the mixed precipitation band.

The version of the snow model presented in this paper contains two major changes relative to the version presented in Martinez et al. (2010). First, melt occurs only in the mixed portion of the snow/rain precipitation interval ($f > T > f\text{-}dif$). This is due to the second model modification: no snow falls or exists in snow pack form when $T>f$. Martinez et al. (2010) allowed snow pack (*A*) to diminish slowly through the spring, completely dependent on parameter *e*. We found that spring peak flow was diminished because snow pack could not melt fast enough and enter the ABCD portion of the model as P_{eff}. To address this issue, we forced any snow pack stored in *A* to completely melt once $T>f$. Figure 7 compares distributions of daily snow pack amount in a given month with the distributions of monthly average temperatures from those months. Results from Figure 7 suggest this snow melt modelling approach is appropriate given that snow pack rarely transfers from April into May for much of this region, and in fact, almost all snow pack entering April from March will melt and contribute to April runoff, a month that commonly has monthly average temperature well above parameter *f* values for our demonstration models. A detailed description of each snow model parameter is provided below.

State Variables

State Variable 'Frac'

Model parameter *Frac* represents the fractional amount of precipitation falling as snow or rain. It is bounded between zero and one and is defined as: $Frac = (f\text{-}T)/dif$. As *T* approaches the value of *f*, *frac* approaches zero, indicating small amounts of precipitation falling as snow. Conversely, as *frac* approaches the value *f-dif*, *frac* approaches the value one, resulting in P_{tot} falling predominantly as snow. Model parameter *Frac* is only used when *T* is in the range $f > T > f\text{-}dif$.

State Variable 'A'

The snow model accumulates snow pack and accounts for changes in snow pack amount in each time step *T* is less than *f*. This accumulation of snow pack is represented in the model as parameter *A*. When *T* is less than *f-dif*, all incoming P_{tot} is accumulated into *A* as snow pack. When *T* is in the range *f* > *T* > *f-dif,* a portion of the incoming P_{tot} will be accumulated as snow pack as defined by the *frac* parameter, and when *T* > *f,* all snow pack stored in *A* is released as melt, in parameter *mt* and contributes to the P_{eff}.

State Variable 'mt'

Total melt from model snow pack (*A*) occurs in the range *f* > *T* > *f-dif*. Melt (*mt*) is defined as: $mt = (A[i-1] + P_{tot}*Frac)*e*Frac$, here the previous time steps snow pack (*A[i-1]*) summed with the fraction of total precipitation falling as snow in the current time step ($P_{tot}*Frac$), multiplied by the product of the melt factor and the snow fraction (*e*frac*). Under this formulation, melt is a monotonically increasing function from *f-dif to f*, with a discontinuity typically at *f* as any snow pack left in *A* is released once *T* is above *f* (see the melt value in Figure 6).

Calibration Parameter 'e'

Parameter e dictates the rate at which melt occurs. Parameter e is only a controlling factor in determining effective precipitation when the monthly average temperature, *T*, is within the range of:*f*> *T* >*f-dif*, which coincides with the mixed precipitation zone. In previous formulations of the model, melt occurred during periods where monthly average temperature, *T*, is above *f*. Our formulation of the model assumes when *T* is above *f*, all snow pack (*A*) from the previous timestep melts and enters the ABCD model as P_{eff}.

<u>*Calibration Parameters*</u>

Calibration Parameter 'f'

Parameter *f* represents the upper bound at which snow occurs. In previous formulations, *f* represented the upper limit of the range where mixed precipitation began. In the current formulation, when *T* (monthly average temperature) is above *f*, all precipitation entering the system falls as rain and any snow present from previous time steps melt and contribute to the effective precipitation (P_{eff}) in the current time step (see right side of Figure 5).

Calibration Parameter 'dif'

The *dif* parameter represents the width of the range in which precipitation can fall as a mixture of snow and rain. The value of *f-dif* represents the lower bound of this range. Anytime *T* is below the *f-dif* value, all incoming precipitation enters as snow, and no melt occurs (see left side of Figure 5).

4.1.2 Driving Data

Two primary data sources are used as input to the ABCDE model: gridded historic meteorological data developed by Maurer et al. (2005) and USGS stream gage records obtained via the NWIS database.

Gridded Meteorological Data

The meteorological forcing data for the ABCD model is derived from the 1/8th degree data product developed by Maurer et al (2005). This dataset contains daily estimates of maximum daily temperature (Tmax), minimum daily temperature (Tmin), and cumulative daily precipitation (Prcp), as well as wind speeds. Tmax, Tmin, and Prcp are the meteorological forcings needed to derive the inputs for the ABCD model. The period of record for this dataset is 1949-2010. The ABCD model takes in average monthly temperature (T), cumulative monthly precipitation (P), and an estimate of the monthly evapotranspiration (ET). For each basin, the following steps are used to produce the needed inputs:

1. Identify the gridcells within the watershed boundaries and extract daily Tmax, Tmin, and Prcp
2. Aggregate the Tmax, Tmin, and Prcp to a monthly timestep. Average Tmax and Tmin to create T
3. Pass Tmax, Tmin, and the basins centroid latitude to the Hargreaves function to create ET
4. Return T, P, and ET as an input file and pass to the ABCD model.

The Hargreaves function is a simple method to take monthly Tmax, Tmin, and the latitude of a watersheds's centroid and convert them in potential evapotranspiration. A more detailed description of the Hargreaves function (Hargreaves and Somani, 1985) can be found in the appendices of this document.

USGS Stream gage Data

The United States Geological Survey (USGS) maintains surface water gages at over 9,400 locations across the United States in real time and have archived data for over 25,000 surface water sites. Most of these gages record streamflow (discharge), with data made available via the NWIS server (http://waterdata.usgs.gov/nwis/sw). USGS gage data serve as our 'dependent variable', which the ABCD model parameters are calibrated to. To generate a dependent variable set, daily discharge data recorded within a basin of interest are aggregated to a monthly timestep and converted into millimetres of runoff per month. These data are passed into the ABCD model and the MCMC sampling method selects distributions of the calibration parameters that minimize error between model and observed streamflow.

Observed streamflow can be used as an evaluation tool for assessing the models ability to accurately capture the seasonal variation in timing and amount of discharge. This study is currently using fifteen basins and USGS gaging stations of interest within the Connecticut River watershed to assess overall model performance.

4.1.3 Bayesian Framework and Hierarchical Setup

This section describes how the ABCD model is formulated in a Bayesian framework, first as a single basin example, and then again as a hierarchical model.

4.1.3.1 Bayesian Framework

Bayesian methods provide a formal mechanism to characterize the error in hydrologic model predictions that stem from uncertainties in model parameterization, structure, and calibration data. In the Bayesian framework, previous knowledge about each parameter value can be incorporated into model calibration through a probability density function known as the prior distribution. A likelihood function is then used to summarize the distribution of model errors, and Monte Carlo Markov Chain sampling procedures can be used to characterize the posterior distributions of hydrologic and error model parameters. If the likelihood function correctly represents the sampling distribution of model errors, parameter and predictive uncertainties can be integrated to develop confidence bounds for streamflow estimates.

Let a conceptual rainfall runoff model be formulated as follows,

$$Q_t = f\ \theta, X_t\ + \varepsilon_t,\ t = 1,2,\dots n \qquad (1)$$

where Q_t equals the observed streamflow at time step t, $f(*)$ represents the streamflow model prediction, θ equals the set of hydrologic and error model parameters, X_t equals the input data at time t, ε_t equals model error, and n represents the number of time steps. Here we assume that all errors associated with input data measurements, response data measurements, and model structure are aggregated into the error term ε.

Before proceeding with calibration, all previous knowledge about each hydrologic and error model parameter is summarized in a prior distribution, denoted $P(\theta)$. If no prior information is available, non-informative priors can be used so that calibration is driven by observed data only. The likelihood function, $L(Q|\theta)$, is defined to match the sampling distribution of ε and is essentially a measure of model skill. Bayes' Theorem can then provide the posterior distribution of model parameters,

$$P\ \theta|Q\ = \frac{L(Q|\theta)\times P(\theta)}{(L(Q|\theta)\times P(\theta)\times d\theta)} \qquad (2)$$

The integral in the denominator is a constant of proportionality required to ensure that the right hand side term is a well-defined probability density function. A unique advantage of the Bayesian framework is that the value of additional data is explicitly accounted for in model calibration. That is, if little data exist for model calibration, the priors will dominate the determination of parameter posteriors, but influence over the posteriors shifts to the likelihood as additional calibration data is made available. This has significant implications for climate change impact assessments. If little data exist for model calibration and no prior information about parameter values is available, the uncertainty of model parameterization is high and any differences between historic and future hydrology simulated by the model under climate change are questionable. The Bayesian scheme can account for these factors, providing a mechanism for more formal comparisons between projected climate and baseline hydrologic regimes.

To calculate confidence bounds on a future streamflow prediction, uncertainty in both model parameters and predictive skill need to be integrated as follows [Stedinger et al., 2008],

$$P\left(\bar{Q}_h \mid Q\right) = \int P(\bar{Q}_h|\theta) \times P(\theta|Q) \times d\theta \qquad (3)$$

where $\bar{Q}_h = f(\theta, X_h)$ equals a future prediction of streamflow at time step h and Q equals all previous observations of streamflow prior to h. Here, the probability distribution of a future streamflow prediction is equal to the product of the likelihood function and the posterior distributions for hydrologic and error model parameters, integrated over the entire parameter space. If hydrologic and error model parameters are distinguished as θ_M and θ_ε, respectively, then predicted percentiles, $\bar{Q}_\alpha$, for the exceedance level 1-α can be constructed for a future prediction at time h as follows [Schoups and Vrugt, 2010],

$$P\left(\bar{Q}_h \leq \bar{Q}_\alpha \mid X_h\right) = P\left[f\left(\theta_M, X_h\right) + \varepsilon(\theta_\varepsilon)\right]_{1,\ldots,J} \leq \bar{Q}_\alpha = \alpha \qquad (4)$$

where $\varepsilon(*)$ is the error model and J is the number of parameter sets sampled from the posterior parameter distributions. J samples of model estimates, $f(\theta_M, X_h)$, and model errors, $\varepsilon(\theta_\varepsilon)$, are added together to produce a cumulative distribution function of predicted values from which the predicted percentile can be inferred. Then, $[\bar{Q}_{0.025}, \bar{Q}_{0.975}]$ forms a 95% confidence bound around the future streamflow estimate $\bar{Q}$. If $\varepsilon(*)$ is set to zero, then prediction error associated with hydrologic model parameter uncertainty can be isolated.

4.1.3.2 Hierarchical Setup

For multiple basins, we consider estimating parameters across space, allows ungage4d location estimation. The hierarchical framework will allow explicit accounting for differences in land use between basins, and readily uses changes in land use generated from external models in calculation of streamflow. This work is currently in progress and is expected to be near completion by the beginning of 2012.

4.1.4 Climate Change Analysis

The climate change analysis uses the ABCD and snow models from above, but replaces the historic forcings they were calibrated with, with projections of temperature and precipitation from global climate models. For this work, we rely on the World Climate Research Programme's (WCRP's) Coupled Model Intercomparison Project phase 3 (CMIP3) multi-model dataset as the foundation for the climate change analysis. These data are on the same grid as the historical meteorological data and contain downscaled monthly temperature and precipitation projections for 112 IPCC climate change scenarios. These data are transient time series, that is, the meteorological data begin in 1950 and evolve according to global climate response to anthropogenic emissions, through 2099, providing 150 years worth of temperature and precipitation estimates for each climate scenario. This ensemble of climate data is used to categorize and quantify the uncertainty in climate model projections.

For an individual basin, all or a selected number of climate change projections can be passed through the ABCDE model to yield projected estimates of streamflow.

Seventy-three transient future climate simulations, running from 1950 to 2100, and sampled across the A1b, A2, and B1 emission scenarios, were gathered from the World Climate Research Programme's (WCRP's) Coupled Model Intercomparison Project phase 3 (CMIP3) multi-model dataset. GCM simulations were downscaled according to the bias-correction and statistical downscaling (BCSD) approach described in *Maurer et al. [2007]*. Thirty year climate windows centered around 1965 were considered baseline conditions for each GCM scenario. For each GCM simulation, a future climate scenario were taken from thirty-year windows of downscaled climate data centered around the year 2075. The historic range of the monthly average maximum and minimum temperature was applied to the projections of average monthly temperature to generate projected maximum and minimum monthly temperatures, as monthly maximum and minimum temperatures were not downscaled from the climate models.

4.2 Stream Temperature Model – Nonlinear Regression Model

The stream temperature model is a nonlinear model formulated by Mohseni et al. (1999). The stream temperature model is dependent on five parameters, three of which are derived from the driving data. Monthly and weekly stream temperatures are highly correlated with ambient air temperature (Mosheni et al. 1999), making projected changes of ambient air temperature a useful predictor for changes in stream temperature due to climate change (Mosheni et al. 2003). A statistical technique developed by Morrill et al. (2005) can be used to translate projections of future climate directly into stream temperature forecasts under future climate scenarios.

Our approach uses the same framework as the Morrill et al. study (linear and nonlinear regression techniques), but examines whether basin specific regression models or a 'universal' model constructed using hierarchical Bayesian model yields more robust model parameters, and thus more scalable results. This method will be calibrated and then verified for our study sites using all available water temperature data within the NALCC.

This approach complements ongoing stream temperature collection efforts being conducted by the USGS as part of their ambient monitoring programs (National Water Information System) and those of the USFS, including ongoing work in Virginia and other East Coast locations (Trumbo et al. 2011). However, the required data for thorough model verification may not be available at many sites within the NALCC.

4.2.1 Model Details

The stream temperature model defined by Mohseni et al. (1999) is composed of two parameters that will be estimated in the MCMC, β, which represents the air temperature at the inflection point of the non-linearity, and γ, which determines the nonlinear rate at stream temperature varies with air temperature. The model is formally defined as:

$$T_S = \frac{\alpha}{1+e^{\gamma(\beta-T_a)}} \qquad (5)$$

, where T_s is defined as the estimated stream temperature,

Something here on how Bayesian approach can use any data available!

4.2.2 Driving Data

4.2.3 Bayesian Framework and Hierarchical Setup

4.2.4 Climate Change Analysis

5 Model Assessment

This section presents assessments of the hydrology and stream temperature models. What follows are applications of these models over broad spatial and temporal scales for validation purposes. Additionally, we examine the impacts of climate change on streamflow and stream temperature, and the role model uncertainty has in defining our ability to determine the impacts of climate change to a riverine system.

5.1 Application of Hydrology Models

The following two sections present an assessment of model skill over multiple basins, including an examination of predicting streamflow at ungaged locations. The first section details model application to the White River basin in Vermont, and provides an in-depth analysis of model uncertainty relative to uncertainty with current climate change projections. The second section is an evaluation of model skill at gaged and 'ungaged' locations. This analysis provides a meta-view of model skill across large ranges of space, climate, and watershed conditions, and the model ability to predict streamflow at ungaged locations.

5.1.1 Application of Statistical Framework in Climate Impact Assessment

The White River is a major tributary of the Connecticut River in New England, draining 1,790 square kilometers in the central, east portion of Vermont (Figure 11). Running 97.6 km from the Green Mountains to the Connecticut River Valley below, the White River is the largest gauged basin in the Connecticut River Watershed without significant regulation from upstream reservoirs or land use changes. Precipitation rates are relatively constant throughout the year, averaging approximately 100 mm/month. Seasonal variations in temperature drive snow accumulation and melt processes that drive hydrologic response throughout the winter and spring months. Streamflow is lowest during the summer and early fall months when evapotranspiration rates reach their peak.

Historic, monthly averages of precipitation and maximum, minimum, and mean daily temperatures were gathered for the basin over the period of January 1980 to December 2005 from the gridded observed meteorological dataset produced by Maurer et al. (2002). Average monthly streamflows were collected from the United States Geological Survey (USGS) West Hartford gauge located at the mouth of the White River. Monthly averages of potential evapotranspiration were calculated using the Hargreaves method (Hargreaves and Samani, 1982). For each calendar month, the distribution of monthly streamflow was examined. All monthly streamflows were log-normally distributed and the seasonally adjusted series exhibited low autocorrelation (lag 1 autocorrelation of 0.17). Also, differences between mean spring and summer flows range across an order of magnitude, as do their standard deviations. Considering these factors, a log-normal likelihood distribution with mean zero and standard deviation σ was chosen to characterize the sampling distribution of model error

$$f(\varepsilon_{ln}) = \frac{1}{\sqrt{2\times\pi\times\sigma^2}} \times \exp\left(\frac{\varepsilon_{ln}^2}{2\times\sigma^2}\right)$$

whereε_{ln} = *ln(Q)-ln($\hat{Q}$)*. The prior for σ was set to an inverse gamma distribution. The posterior of this parameter characterizes the level of uncertainty in hydrologic model estimates.

Past studies were used to inform prior distributions for the hydrologic model parameters *a,b,c,* and *d* (Alley, 1984; Fernandez et al., 2000; Martinez and Gupta, 2010; Vandewiele et al., 1992), and the remaining model parameters were given non-informative priors in the form of uniform or normal distributions. MCMC sampling was used to explore the posterior distributions of hydrologic and error model parameters. The slice sampler was chosen for the MCMC sampling and was implemented in the JAGS programming language [Plummer, 2011]. Three chains were used in the sampling. Calibration was implemented over the period between January 1980 and December 1999, leaving twenty years of data for verification. Table 2 summarizes the prior and posterior distributions for all parameters inferred in the MCMC sampling.

Figure 8(a) presents histograms of the prior and posterior distributions of parameter *a*, and Figure 8(b) shows the history plots of parameter *a* for the three chains. For all model parameters, the Gelmin and Rubin statistic was within 0.005 of 1, suggesting that convergence was reached for all parameters considered.

Figure 8(c) presents a quantile plot of the log-transformed model errors over the verification period (January 2000 to December 2005), and Figure 8(d) shows their partial autocorrelation coefficients. Results from the quantile plot suggest that model errors follow a log-normal distribution, and partial autocorrelation coefficients in Figure 8(d) were deemed small enough to ignore. Therefore, the original choice of a log-normal likelihoodfunction with no autocorrelation component was considered adequate for this modeling exercise. Figure 9shows the observed monthly streamflow for both calibration and verification periods (1995-2005), as well as model estimates generated by the median values of the posteriors for hydrologic model parameters. Also shown are error bounds consistent with the 2.5th and 97.5th percentiles of streamflow estimates. Observed data from the calibration and verification periods fell within the 95% credible interval 3.3% and 6.7% of the time, respectively, again suggesting that the error model adopted is appropriate for this application.

Significance of Future Hydrologic Alteration

Seventy-three transient future climate simulations,running from 1950 to 2100 and sampled across the A1b, A2, and B1 emission scenarios,were gathered from the World Climate Research Programme's (WCRP's) Coupled Model Intercomparison Project phase 3 (CMIP3) multi-model dataset. GCM simulations were downscaled according to the bias-correction and statistical downscaling (BCSD) approach described in *Maurer et al. [2007]*. Thirty year climate windows centered around 1965 were considered baseline conditions for each GCM scenario. For each GCM simulation, a future climate scenario was taken from thirty-year windows of downscaled climate data centered around the year 2075. The historic range of the monthly average maximum and minimum temperature was applied to the projections of average monthly temperature to generate projected maximum and minimum monthly temperatures, as monthly maximum and minimum temperatures were not downscaled from the climate models.

Distributional alterations are considered in the statistical framework for four monthly streamflow averages: January, March, April, and October. These months were chosen because they the exhibit a wide range of changes under future climate and highlight the importance of including hydrologic model error in climate impact assessments.

Figure 12 presents the median, 97.5th, and 2.5th percentiles for quantile estimates of monthly flows for one GCM over a baseline period and future period centered around 2075. Figure 12(a) shows that there are significant differences between the distributions of January flows in the baseline and future periods after accounting for model error. Results suggest that future January flows will be significantly higher in their future, most likely due to a shift in the ratio between rainfall and snowfall driven by increased wintertime temperatures. Over most of the quantile range, the 2.5th percentile of January flow quantiles from the 2060-2090 period exceed the 97.5th percentile of quantiles taken from the historic period. This suggests that under this particular GCM climate projection, future increases in January flows can be attributed to future climate shifts and not just hydrologic model error. We note that the uncertainty bounds of the baseline and future scenarios begin to overlap towards the extreme quantiles, suggesting that the hydrologic model is less capable of predicting changes to the most extreme January monthly flow events. This is likely due to the scarcity of extreme data points available during calibration.

Figure 12b and Figure 12c show results for March and April average streamflows, respectively. Results indicate that March flows will increase in the future while April flows will decrease below their historic norms. These changes are driven by earlier snowmelt occurrences in the spring and decreases in snowpack storage that historically have persisted into the later spring. Interestingly, the highest 10% of March flows show no significant departures from historic values (Figure 12b); differences become significant for lower flows below the 30% quantile, where median quantile estimates in the future period begin to exceed the 97.5thpercentile quantile estimates from the historic period. A similar pattern is seen for April flows (Figure 12), although significant differences emerge between historic and future flow quantiles for even some of the highest flows. For some of the highest quantiles, median estimates for the future period drop below the credible interval bounds of the baseline period. However, changes in April flows are still much more significant for lower quantiles. Credible intervals for baseline and future estimates of the 50% - 80% quantiles show almost no overlap, suggesting that climate-impacted flows are truly different than the baseline.

Figure 12d shows results for the month of October. There are no significant differences between future and baseline October flows. Median quantile estimates are almost identical, and credible intervals for the two time periods show significant overlap.

The statistical framework can also be used to assess the significance of future hydrologic alterations across an ensemble of GCM projections. Figure 13shows the median quantile estimates of monthly flows over a baseline period and an ensemble of future periods, along with the associated credible interval for the baseline estimate. This figure facilitates a comparison between uncertainties in future hydrologic alteration stemming from the hydrologic model and the GCMs. Figure 13a shows that all GCM simulations exhibit a similar upward trend in January flows as those discussed previously, and many median future estimates lie outside the credible interval for the baseline period. Figure 13a also shows that the uncertainty associated with the GCMs, as represented by the spread of January quantile estimates, is much larger than the uncertainty associated with the hydrologic model. That is, the contribution of hydrologic model error to the cumulative uncertainty surrounding future January flows is small when compared to uncertainties associated with future climate projections. This is not the case with March, April, and October flows. For March, all GCMs indicate a significant, upward trend in future flows, but the spread of GCM predictions is comparable to the spread in hydrologic model uncertainty (Figure 13b). A similar pattern is seen for April flows, except the trend is downwards (Figure 13c). For October, there is no trend in future flows and the median GCM projections of flow quantiles are almost completely bounded by the baseline credible interval.

Finally, uncertainties from the hydrologic model can be combined with those of future climate simulations to explore the full range of uncertainty associated with the future hydrologic projections under consideration. This is shown in Figure 14, which is identical to Figure 13 except for the addition of a credible interval for the GCM ensemble, depicted by the shaded grey area. This credible interval can be constructed by taking the 97.5^{th} and 2.5^{th} percentiles of quantile estimates for monthly flows associated with the upper and lower end-members of the ensemble, respectively. For all months considered, hydrologic model uncertainty is rather insignificant when compared to the spread of GCM ensemble members for lower flow quantiles. However, hydrologic model error becomes equally if not more important than future climate projection uncertainty for the highest flow quantiles. This reflects the difficulties of high flow prediction that plague the current model under consideration. The ability to contrast the uncertainties of the hydrologic model and future climate projections provides key insight into what information about climate-altered hydrology can be garnered from the current model. In this instance, the hydrologic model does not inhibit an analysis of the magnitude of future alterations to low monthly flows, but its inherent uncertainty does prohibit a similar analysis for the largest monthly flow events.

Influence of Hydrologic Modelling Skill on Significance Testing

The hydrologic model considered above exhibited high skill, with errors mostly ranging between 0% and 15% of observations. This skill was manifested in the relatively narrow confidence bounds for future streamflow predictions, especially for low flow periods (Figures 9,12, and 13). If the hydrologic model had greater difficulty replicating observed streamflow, or less data existed for calibration, theory would suggest that model and parameter uncertainty would increase and confidence bounds would widen.

To test this hypothesis, the posterior distribution of σ was artificially shifted upwards by a constant value of 0.8 to simulate decreased model skill. By adding 0.8 to all posterior samples of σ, errors were augmented by an additional 80%. The analysis from Section 4.5 was repeated with the new, degraded hydrologic model, and results for hydrologic alteration under an ensemble of future climates are presented in Figure 15.

When model skill is degraded, the confidence in baseline streamflow estimates is low, resulting in wide uncertainty bounds for all months considered. For January, future streamflows are no longer well above the 97.5th percentile of baseline flow quantiles as they were in Figure 13, especially for the highest flows (Figure 15a). This is even more pronounced for March, where uncertainty bounds for the baseline almost completely envelop future streamflow estimates (Figure 15b). This is starkly different than previous results that suggested future March streamflows were significantly larger than baseline levels. A similar result is seen for April (Figure 15c) and October (Figure 15d). For all months considered, error bounds widen the most for the highest flow quantiles. This stems from the log-transformation of model errors dictated by the lognormal likelihood function. By log-transforming the residuals, errors become multiplicative in nature, such that an error term applied to future high flow estimates is significantly greater in absolute terms compared to the same percent error added to future low flow estimates.

It is important to note that when model errors are increased, there are no changes in the direction of future streamflow alterations. That is, if January flows increased with little model error, they will also, on average, increase when model error is artificially increased. Including hydrologic model uncertainty bounds provides no new information regarding the type of hydrologic alteration that might happen under future climate scenarios. The benefits of formal confidence bounds rest in their ability to quantitatively compare the uncertainty arising from the hydrologic model and future climate projections. This enables analysts and managers to understand the sources of uncertainty underscoring their decisions about climate change adaptation strategies and help identify further courses of action needed to reduce these uncertainties. For example, if future climate projections are relatively consistent in terms of the magnitude and direction of hydrologic alteration, but hydrologic model skill is low, investments should be made in better hydrologic modeling to understand the likely extent of future hydrologic alteration with more precision. Conversely, if the hydrologic model has significant skill but the spread in future climate projections is wide, no additional benefit for decision making will be gained by enhancing the hydrologic model.

There is a growing recognition that advancements in climate change alteration studies are required to inform water resource planners and managers of the magnitude and sources of uncertainty in future hydrology projections. A comprehensive statistical framework that provides this information was presented here. The approach considered was able to propagate uncertainty from a hydrologic model into future streamflow projections and isolate it from uncertainty in future climate projections, allowing for the two sources to be compared. The method does not provide new information regarding the possible direction of hydrologic alteration, but rather facilitates a quantitative analysis of the confidence that can justifiably be afforded to the projected magnitude of such changes.

The application to the White River Basin demonstrated that the framework can highlight the different levels of hydrologic uncertainty across a spectrum of flow quantiles and seasons. If an appropriate likelihood function is chosen, this analysis can identify whether there is more or less evidence of significant hydrologic alteration for different times of year and levels of flow. Distinguishing between the uncertainties in alteration for a range of events and seasons may be of critical importance to the future management of water resources facilities because the vulnerabilities of these systems often vary with the magnitude and timing of streamflows. The methods presented here provide a simple way to express varying levels of confidence in future hydrologic events to planners so they may better understand the worth of different alteration strategies.

5.1.2 Application of Statistical Framework in Modelling Ungaged Basins

5.2 Application of Stream Temperature Models

5.2.1 Application of Stream Temperature Model in Headwater Systems

Index

6 Alternatives Considered and Rejected

Prior to selecting the ABCDE hydrology and stream temperature model, we evaluated alternative methods for generating streamflow and stream temperature: 1) Distributed Hydrology Soil Vegetation Model (DHSVM), 2) Variable Infiltration Capacity (VIC), and 3) the regression approaches for stream temperature.

6.1 Alternative Hydrology Models and Approaches

6.1.1 Distributed Hydrology Soil Vegetation Model (DHSVM)

DHSVM is a distributed hydrology model that incorporates high resolution spatial data (30-150 meter pixels) of land features (land use, digital elevation models, soil maps, etc.)with temporally fine meteorological forcings (3 hourly temperature, precipitation, and wind speeds) to simulate the water budget. It was developed at the University of Washington (Wigmosta et al 1994) as a research tool to investigate hydrology in topographically complex terrain. Water moves between pixels above and below the ground surface following overland flow, unsaturated and saturated subsurface flow theory. Water movement and evapotranspiration can occur from a variable number of soil layers (typically 3), with evapotranspiration dependent on properties of vegetation within a grid cell, land surface properties (aspect, shadowing, and other relevant factors), and the prevailing

meteorological conditions. Water entering a stream channel is routed using kinematic wave approaches.

The fine resolution of the model serves as both the advantage and disadvantage of it relative to ABCDE. DHSVM is capable of modelling sub-daily flow and stream temperature accurately regardless of stream size or location, in addition to modelling water balances and movement in every pixel within the model domain. The model is formulated in accordance with our best understanding of the physics governing water movement and energy budgets within a watershed. Producing high quality results of streamflow and temperature comes at the cost of complex input data needs and long run times. The saying, "a model is only as good as its input data,"rings especially true for DHSVM. It requires accurate and detailed information regarding a watersheds soil characteristics, land use, vegetation types, surficial geology, topography, and stream network in order to construct a model that will yield plausible results. In addition, the meteorological forcingsneeded must be representative of conditions within the basin and temporally disaggregate to produce appropriate storm peaks. Due to the complex data needs, the lack of scalability (not able to create a model for everywhere), and the long run times, DHSVM is only being used in a pilot-mode to verify our ability to model system physics using the ABCDE approach.Add more here from model results

6.1.2 Variable Infiltration Capacity Model

The Variable Infiltration Capacity model (VIC) is a macro-scale, physically based, hydrology model. The spatial resolution of VIC is coarse relative to other hydrology models. VIC was originally developed to represent land surface processes within global circulation models, which tend to operate at scales larger than 2° latitude by 2° longitude, though VIC is now commonly applied to scales ranging from 1/16° to 2°. The spatial resolution of the CRVIC model is 1/8° latitude by 1/8° longitude, or approximately 54 square miles.Add more here from model results

6.2 Alternative Stream Temperature Models and Approaches

6.2.1 Physics Based Stream Temperature Models

6.2.2 Regression Based Models

Index

7 Major Implementation Constraints

7.1 Decision Support System

7.2 Lack of Driving Data

Index

8 Major Risks and Dependencies

8.1 Major risks

Accuracy in ungagged catchments – lack of verification

Simplicity of Model – Different climate change results from other more sophisticated models

8.2 Dependencies

Accuracy of USGS stream gage data

Accuracy of Maurer Wood Historic and project climate data

JAGS and model convergence on correct posteriors

Correct Structural form of model across NALCC region

Ability to delineate a basin correctly and accurately reflect physical conditions within it

Index

9 Acknowledgments

We acknowledge the modelling groups, the Program for Climate Model Diagnosis and Intercomparison (PCMDI) and the WCRP's Working Group on Coupled Modelling (WGCM) for their roles in making available the WCRP CMIP3 multi-model dataset. Support of this dataset is provided by the Office of Science, U.S. Department of Energy.

JAGS dude – Martyn Plummer

USGS – streamflow data

Others?

Index

10 Literature Cited

Archfield, S. A., and R. M. Vogel (2010), Map correlation method: Selection of a reference streamgage to estimate daily streamflow at ungaged catchments, *Water Resour. Res.*, 46, W10513,doi:10.1029/2009WR008481

Bates, B. C., and E. P. Campbell (2001), A Markov Chain Monte Carlo Scheme for parameter estimation and inference in conceptual rainfall-runoff modeling, *Water Resour. Res.*, 37(4), 937–947, doi:10.1029/2000WR900363.

Battin J., M.W. Wiley, R.H. Ruckelshaus, R.N. Palmer, E. Korb, K.K. Bartz, and H. Imaki (2006), Projected impacts of climate change on salmon habitat restoration, *Proceedings of the National Academy of Science*, 104(16), 6720-6725.

Chapra, S.C. (1997), Surface Water Quality Modeling, McGraw-Hill

Daly, C., R.P. Neilson, and D.L. Phillips (1994), A Statistical-Topographic Model for Mapping Climatological Precipitation over Mountanious Terrain, *J. Appl. Meteor.*, 33, 140-158.

Fernandez, W., R.M. Vogel, and A. Sankarasubramanian (1999), Regional Calibration of a Watershed Model, *Hydrological Sciences Journal.*

Letcher B.H., Nislow K.H., Coombs J.A., O'Donnell M.J., Dubreuil T.L., (2007), Population Response to Habitat Fragmentation in a Stream-Dwelling Brook Trout Population, PLoS ONE 2(11): e1139. doi:10.1371/journal.pone.0001139

Hargreaves, G.H., and Z.A. Somani (1985), Reference Crop Evapotranspiration from Temperature, *Applied Engineering in Agriculture*, 1(2): 96-99

Marshall, L., D. Nott, and A. Sharma (2004), A comparative study of Markov chain Monte Carlo methods for conceptual rainfall-runoff modeling, *Water Resour. Res.*, 40, W02501, doi:10.1029/2003WR002378.

Martinez, G. F., and H. V. Gupta (2010), Toward improved identification of hydrological models: A
diagnostic evaluation of the "*abcd*" monthly water balance model for the conterminous United
States, *Water Resour. Res.*, 46, W08507, doi:10.1029/2009WR008294.

Maurer, E.P. (2007), Uncertainty in hydrologic impacts of climate change in the Sierra Nevada, California under two emissions scenarios, *Climatic Change*, 82, 10.1007/s10584-006-9180-9.

Morrill, J C., R.C. Bales, and M. H. Conklin. (2005), Estimating Stream Temperature from Air Temperature: Implications for Future Water Quality. *J. Envir. Engrg*. 131:1(139)

Mohseni O. and H.G. Stefan (1999), Stream Temperature/Air Temperature Relationship: A Physical Interpretation, *Journal of Hydrology*, 218(3-4), 128-141.

Mohseni, O., H.G. Stefan, and J.G. Eaton (2003), Global warming and potential changes in fish habitat in U.S. Streams, *Climate Change,* 59, 389-409.

Thomas, H.A. (1981) Improved methods for national water assessment. Report, Contract WR 15249270, US Water Resources Council, Washington, DC, USA.

Trumbo, B., M. Hudy, E.P. Smith, D.Y. Kim, B.A. Wiggins, K. Nislow, and C.A. Dolloff, (2011), Sensitivity and Vulnerabiltiy of Brook Trout Populations to Climate Change, *Proceedings of Wild Trout X*, West Yellowstone, MT

Vogel, R., (2005), Regional calibration of watershed models, In:Singh, V., Frevert, D. (Eds.), Watershed Models. CRC Press, Baco Raton, FL, pp. 47–71.

Wigmosta, M.S., L.W. Vail, and D.P. Lettenmaier (1994), A Distributed Hydrology Vegetation Model for Complex Terrain, *Water Resour. Res.*, 30(6), 1665-1679.

Wood, A.W., E.P. Maurer, A. Kumar, and D.P. Lettenmaier (2002), Long-range experimental hydrologic forecasting for the eastern United States, *J. Geophysical Research-Atmospheres*, 107(D20), 4429.

Wood, A.W., L.R. Leung, V. Sridhar, and D.P. Lettenmaier (2004), Hydrologic implications of dynamical and statistical approaches to downscaling climate model outputs, *Climatic Change*, 15(62):189-216.

Xu, C., B. H. Letcher, and K. H. Nislow (2010),Size-dependent survival of brook trout *Salvelinusfontinalis* in summer: effects of water temperature and stream flow, Journal of Fish Biology, 76: 2342-2369. doi:10.1111/j.1095-8649.2010.02619.x

Hayhoe, K., C.P. Wake, T.G. Huntington, L. Luo, M. Schwartz, J. Sheffield, E. Wood, B. Anderson, J. Bradbury, A. DeGaetano, T. Troy, and D. Wolfe. 2007. Past and future changes in climateand hydrological indicators in the US Northeast. Climate Dynamics 28:381–407.

Hayhoe, K., C.Wake, B. Anderson, X. Liang, E. Maurer, J. Zhu, J. Bradbury, A. DeGaetano, A. Stoner, andD. Wuebbles2008. Regional Climate Projections for the Northeast. U. S. Mitigation and Adaptation Strategies for Global Change 13: 425-436.

Maurer, E. P., L. Brekke, T. Pruitt, and P. B. Duffy. 2007. Fine-resolution climate projections enhance regional climate change impact studies. Eos Transactions of the America Geophysical Union 88(47): 504.

Wood, A.W., E.P. Maurer, A. Kumar, and D.P. Lettenmaier. 2002. Long-range experimental hydrologic forecasting for the eastern United States. Journal of Geophysical Research-Atmospheres 107: 4429.

Wood , A., L.R. Leung, V. Sridhar, and D. Lettenmaier. 2004. Hydrologic implications of dynamical and statistical approaches to downscaling climate model surface temperature and precipitation fields. Climate Change 62:189–216.

Index

11 Appendix A – Diagrams/Figures/Tables

Table 1: Model Initial Conditions and Calibration Parameter Values Used in Figure 6

Calibration Parameters	Constant Value	Model Parameter	Initial Value
a	0.95	S_{t-1}	50
b	300	P_{eff}	50
c	0.5	ET_{eff}	50
d	0.5		

Table 2: Summary of Prior and Posterior Distributions

Parameter	1st Quartile	Median	Mean	3rd Quartile	Prior Distributions
a	0.982	0.984	0.984	0.986	Beta(a=1.2,b=0.6)
b	303	310	310	316	Normal(mu=300,sd=100)
c	0.14	0.18	0.18	0.22	Beta(a=0.6, b=1.2)
d	0.45	0.66	0.74	0.90	Beta(a=1, b=1)
e	0.141	0.205	0.206	0.268	**B**eta(a=0.8, b=1.8)
f	-1.65	-1.48	-1.47	-1.31	Normal (mu=0,sd=4)
dif	12.9	13.9	14.0	15.0	Uniform(a=0.01, b=20)
ss	0.13	0.14	0.14	0.15	Gamma(shape=1, scale=2.5)

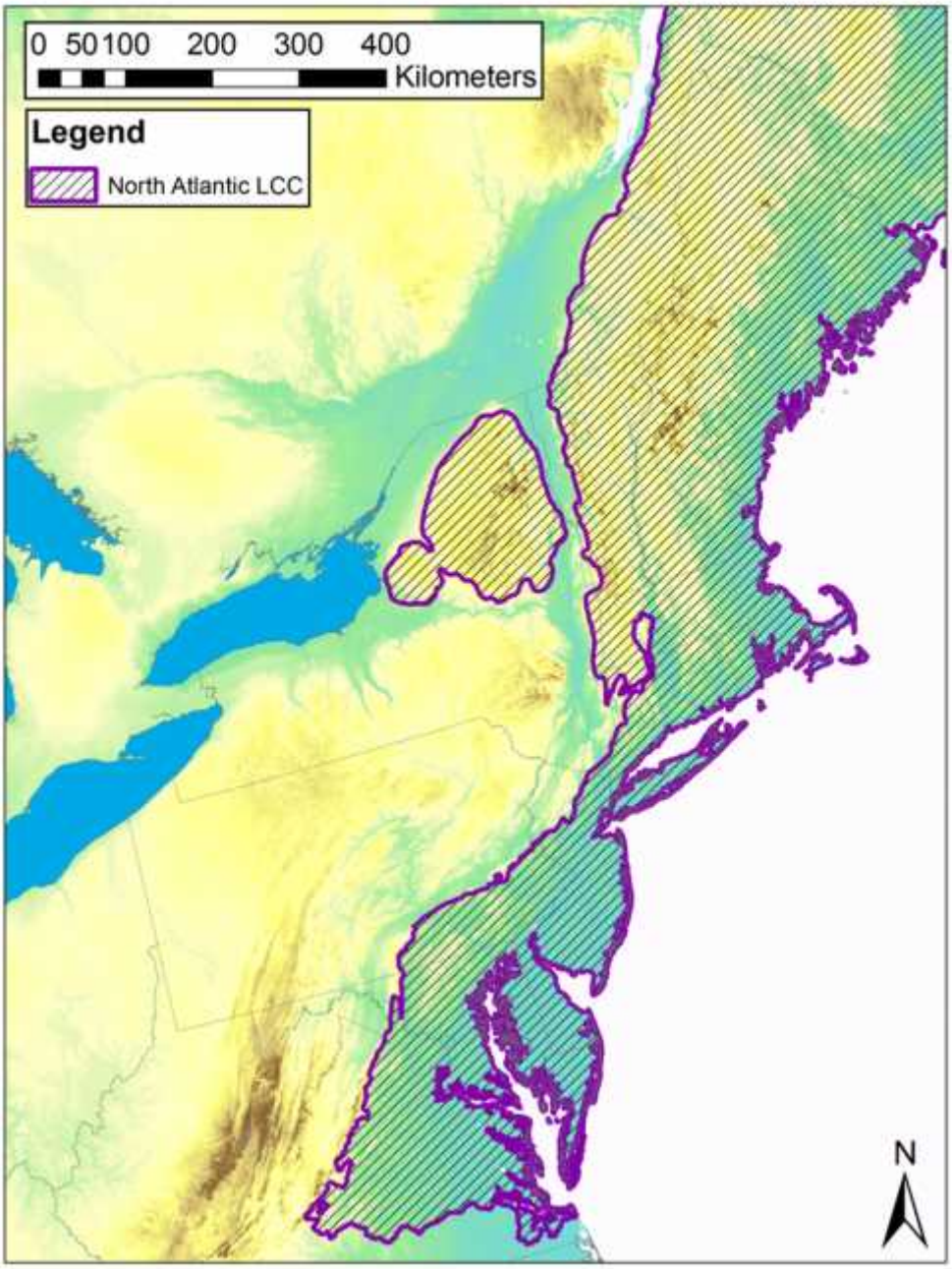

Figure 1: North Atlantic Landscape Conservation Cooperative Region

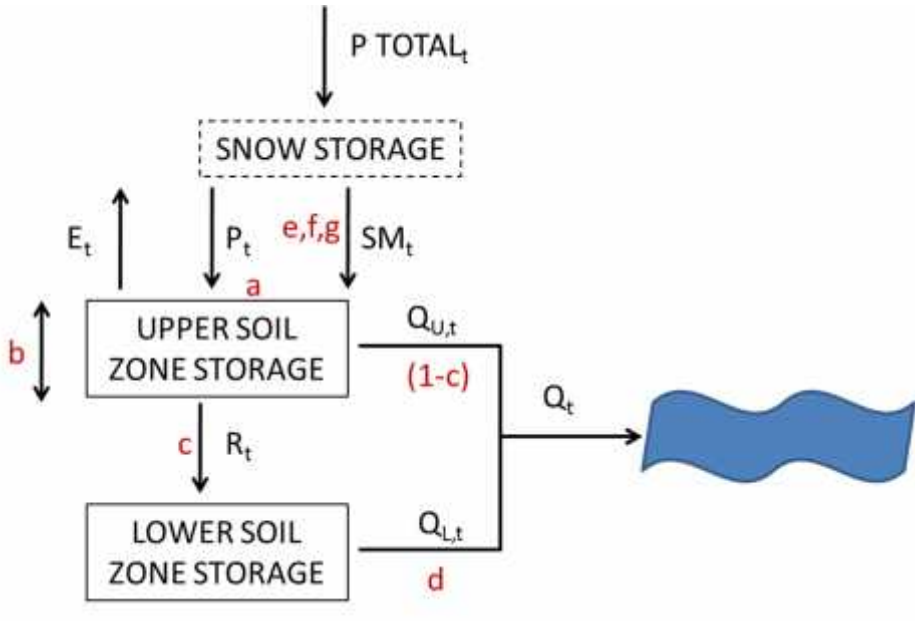

Figure 2: ABCDE Model Schematic

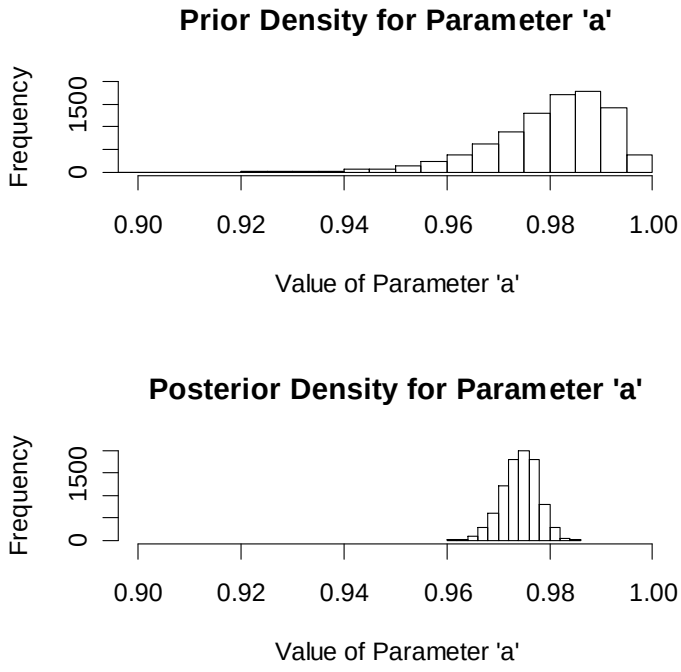

Figure 3: Changing Prior Distribution

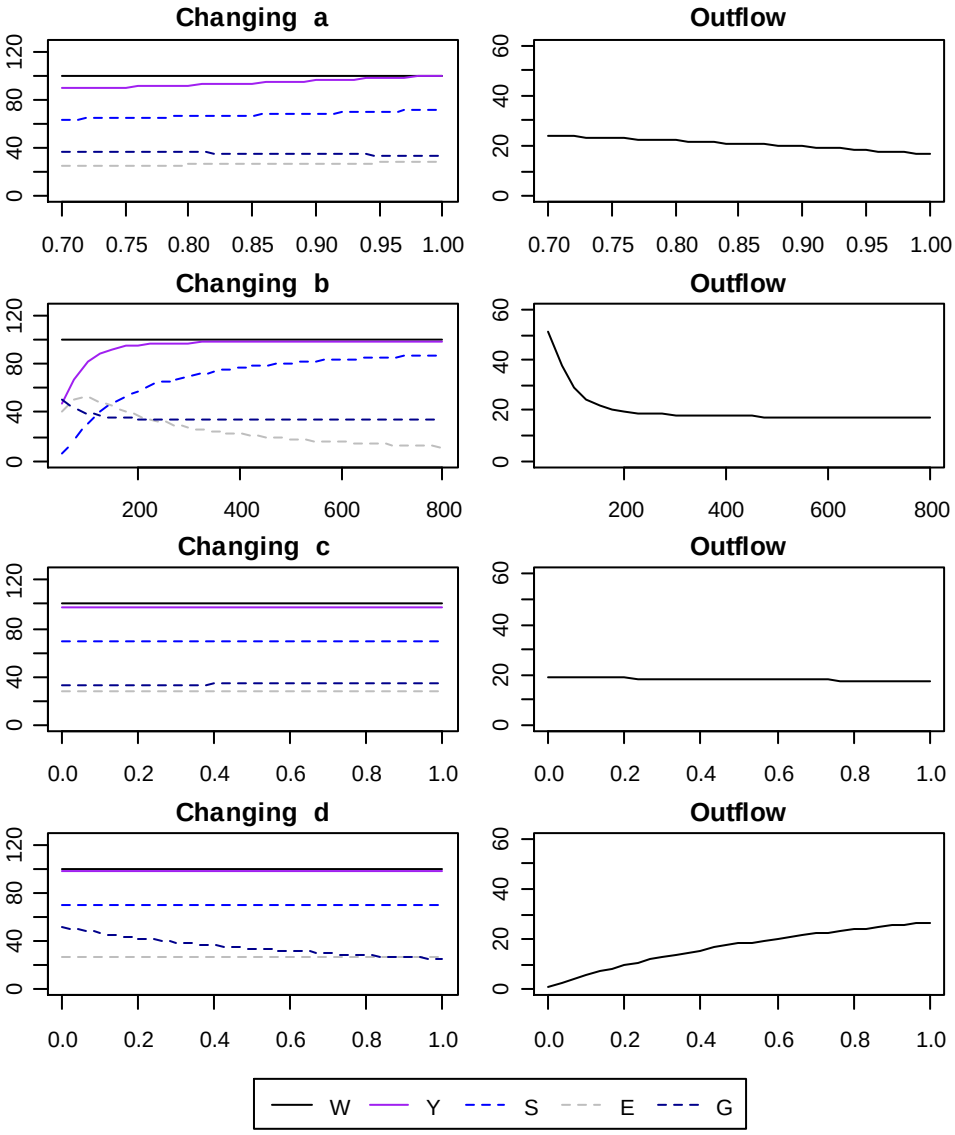

Figure 4: Relationship of Calibration Parameters to ABCD Model Output

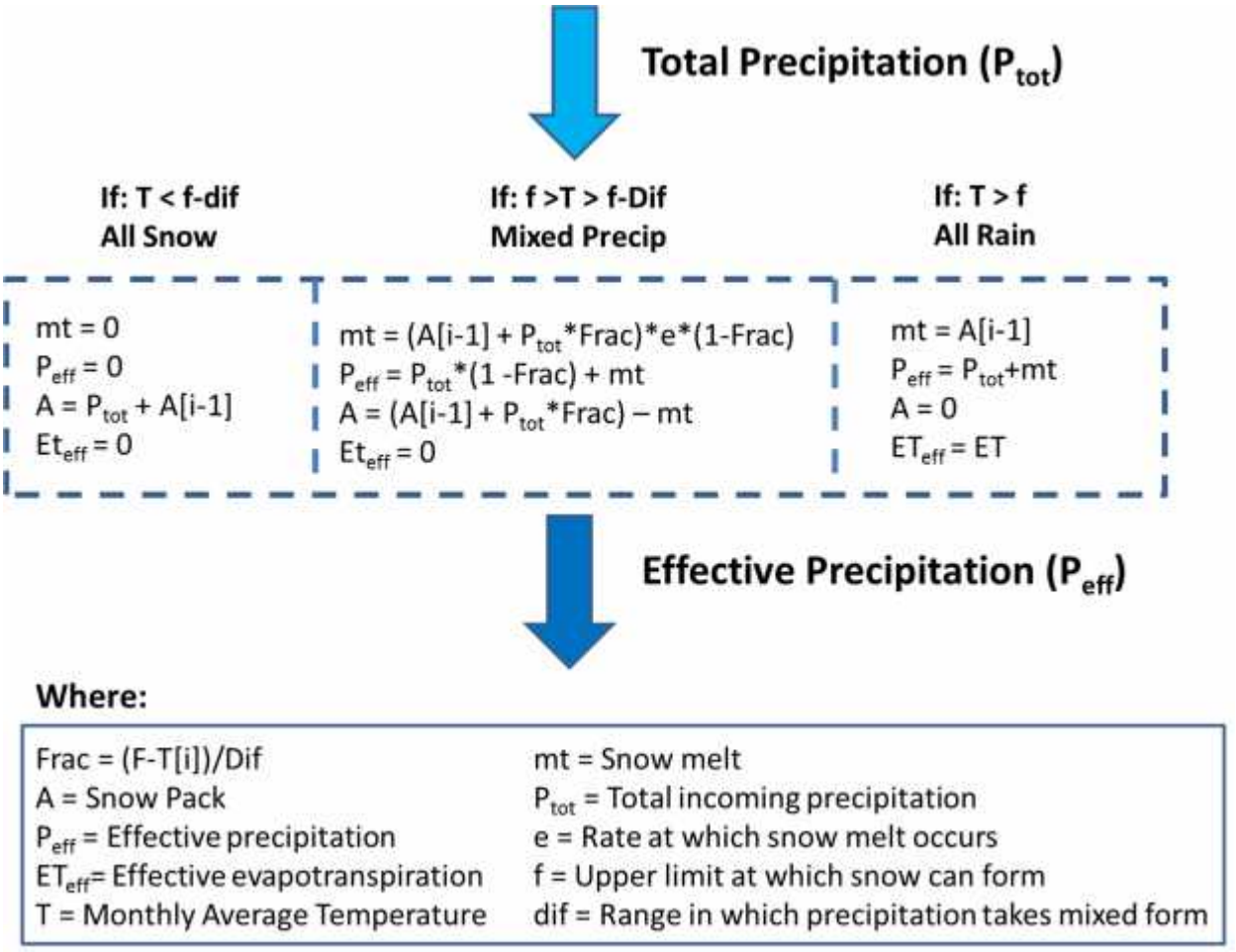

Figure 5: Snow Model Schematic

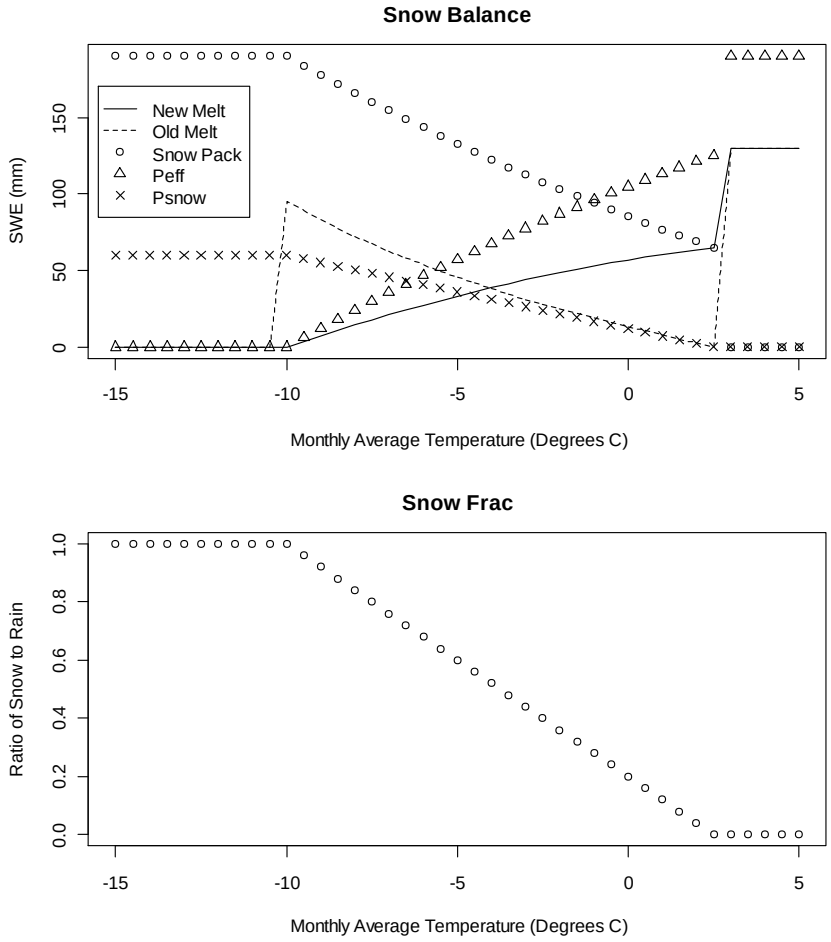

Figure 6: Mass Balance of Water in Snow Model

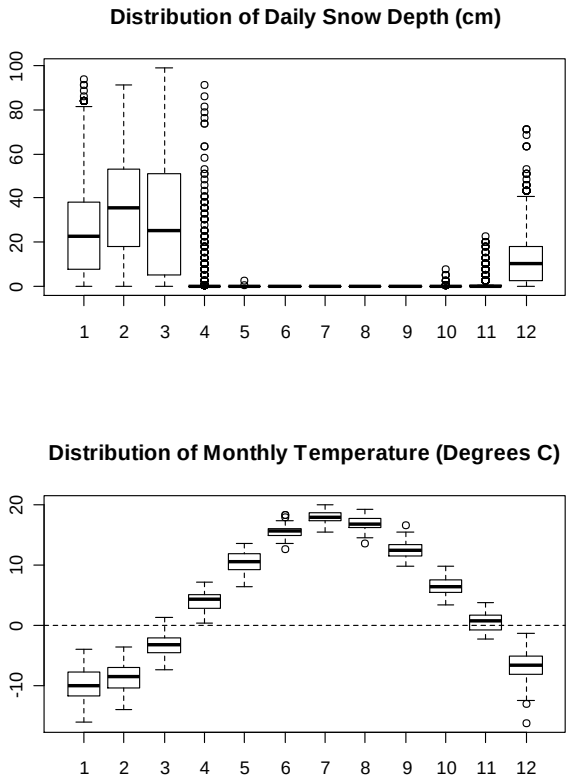

Figure 7: Distribution of Snow Depth and Monthly Average Temperatures

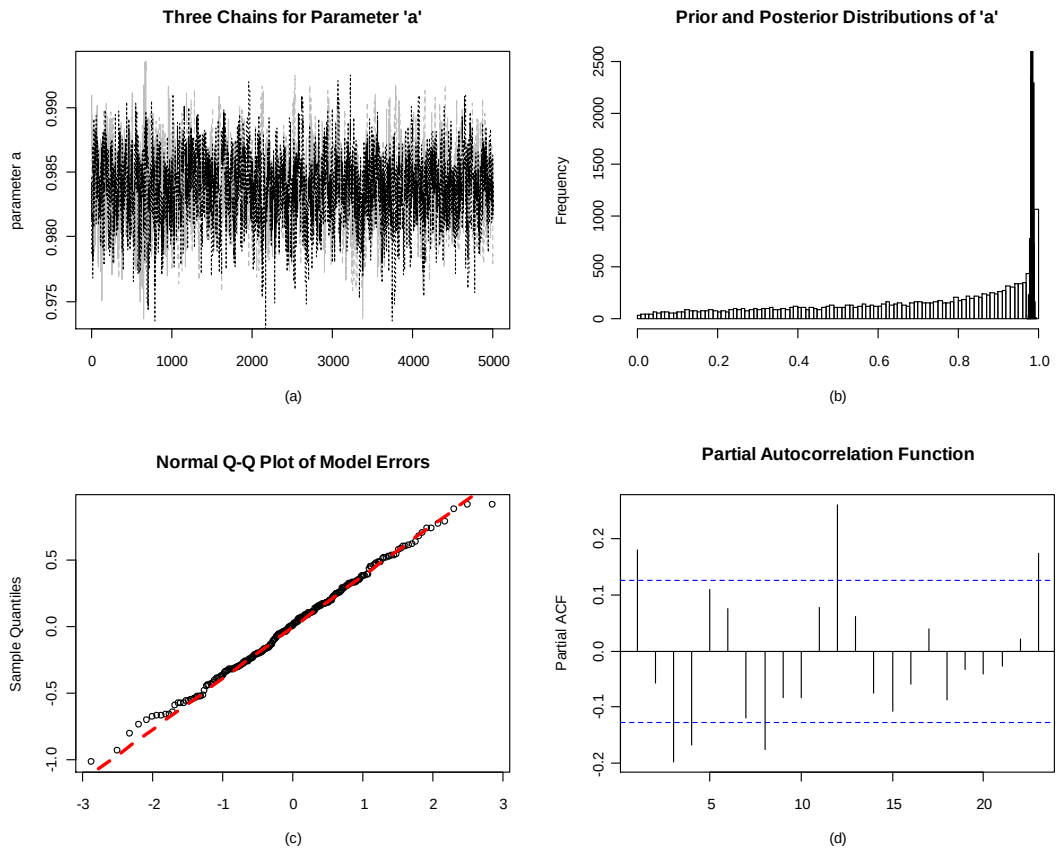

Figure 8: Monte Carlo Markov Chain and Model Error Diagnostics

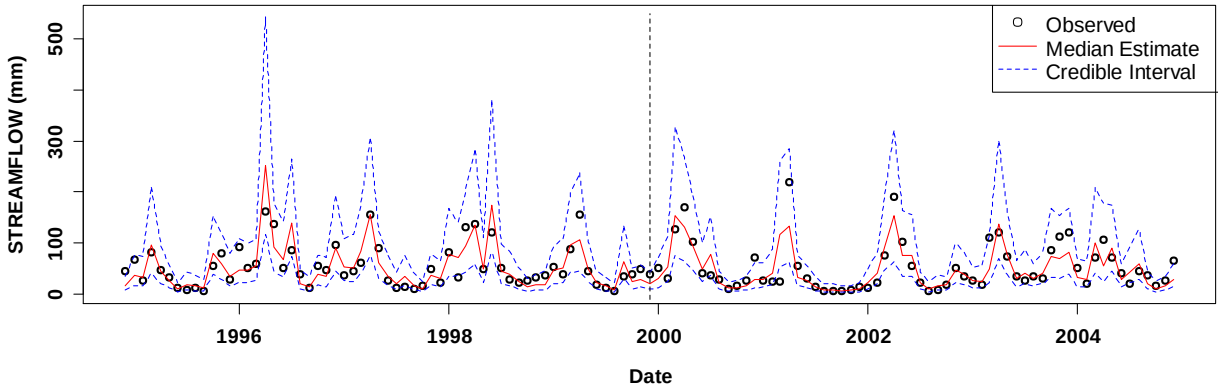

Figure 9: ABCD Model Calibration and Verification Results

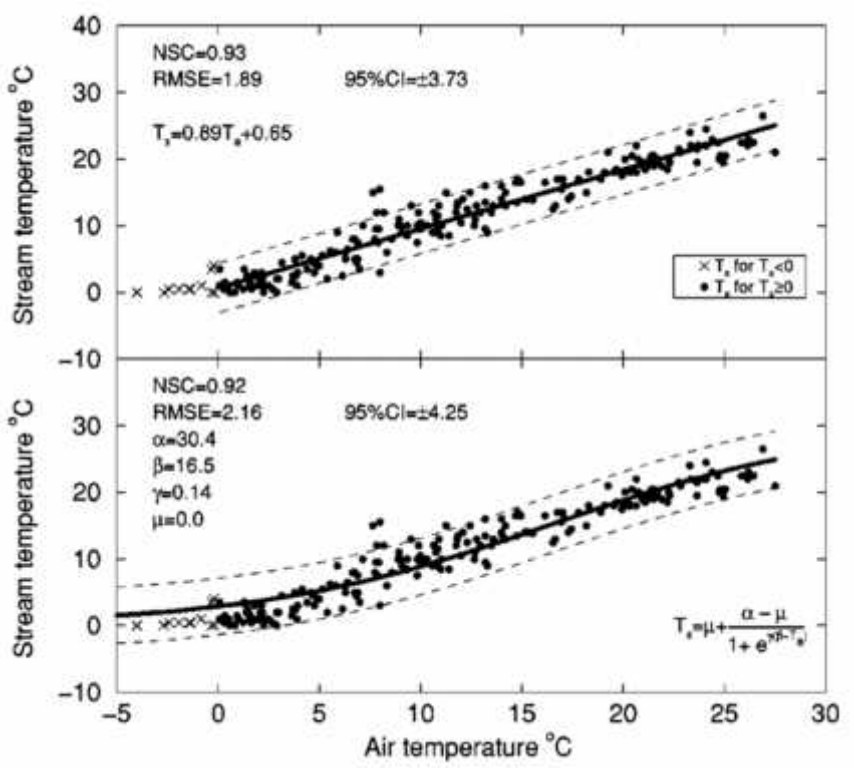

Figure 10: Stream Temperature Model Results

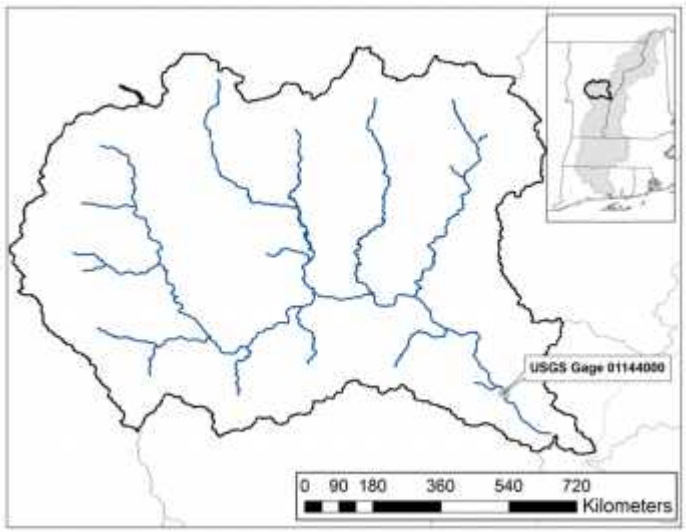

Figure 11: Schematic of the White River Basin - Vermont, U.S.

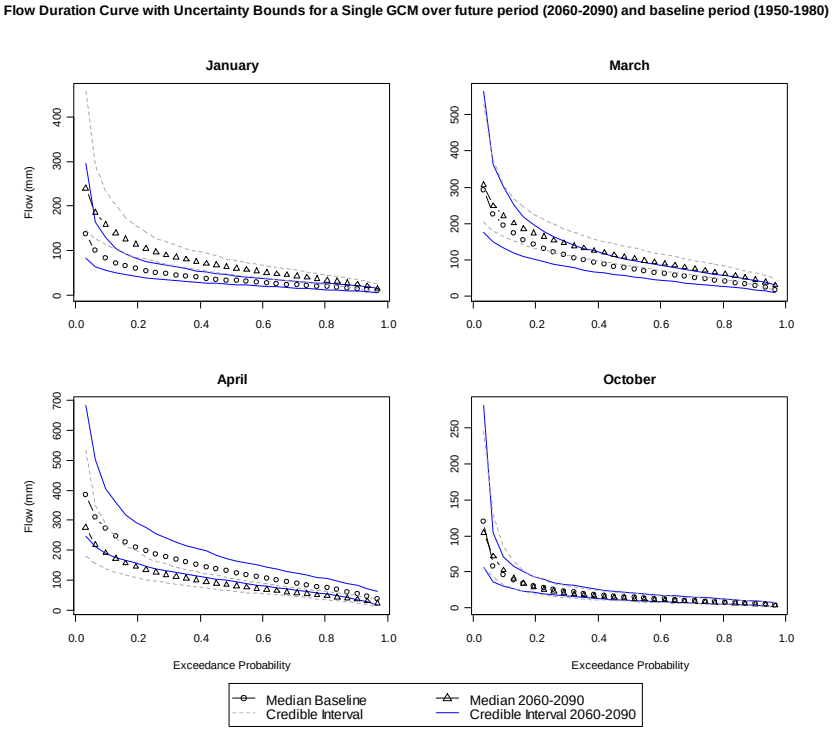

Figure 12: Flow Duration Curve with Uncertainty Bounds for a Single GCM for a Future Period (2060-2090) and a Baseline Period (1950-1980)

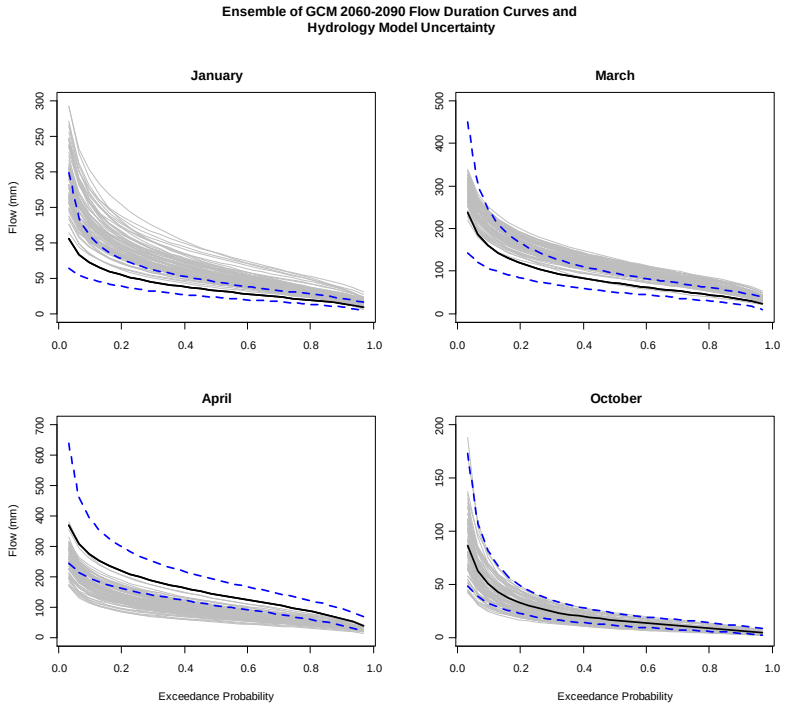

Figure 13: Ensemble of GCM Projections of 2060-2090 Flow Duration Curves and Hydrology Model Uncertainty Bounds.

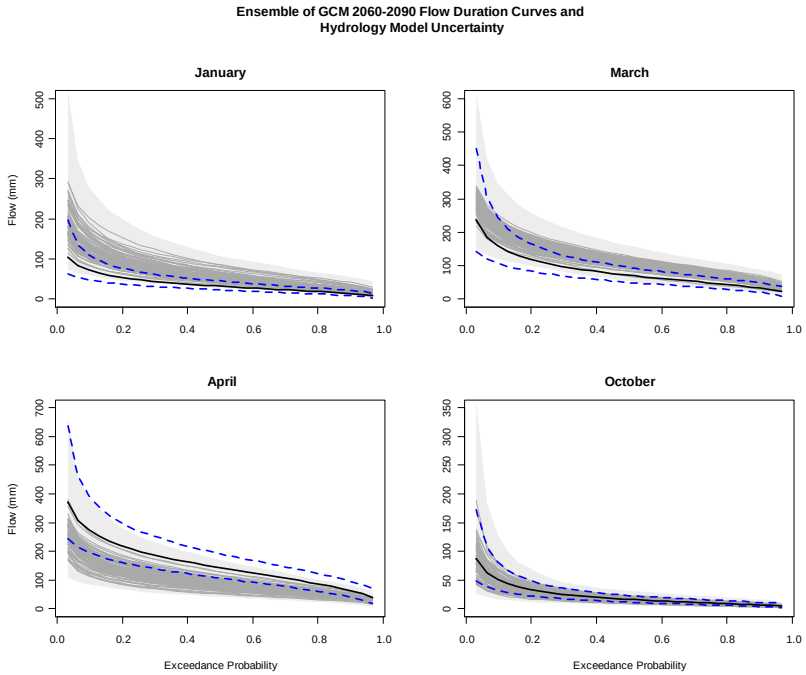

Figure 14: Ensemble of GCM Projections of 2060-2090 Flow Duration Curves and Hydrology Model Uncertainty Bounds With GCM Uncertainty

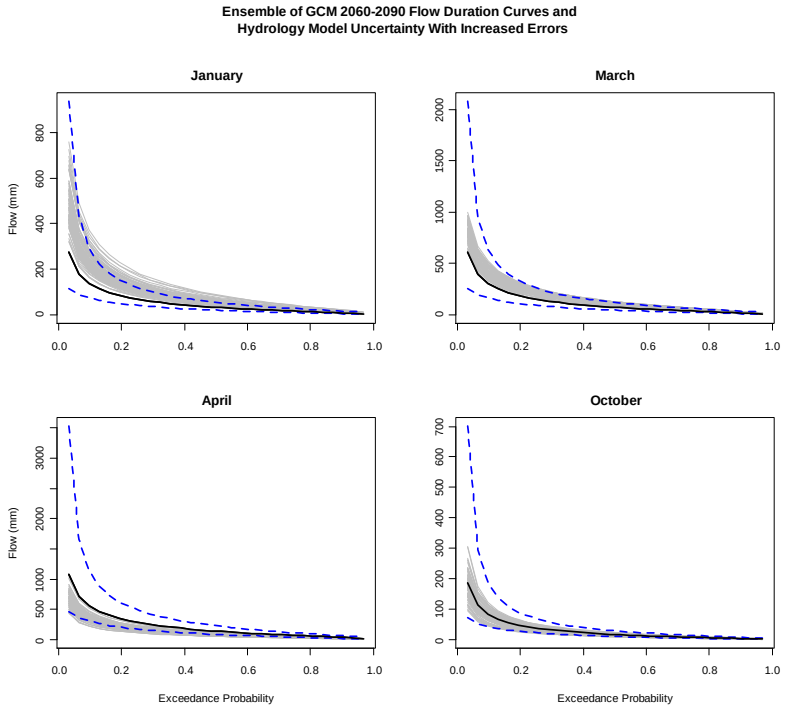

Figure 15: Ensemble of GCM Projections of 2060-2090 Flow Duration Curves and Hydrology Model Uncertainty Bounds With Increased Errors

Index